On the nonlinear anelastic behaviour of AHSS

A Torkabadi, V T Meinders and A H van den Boogaard

University of Twente, P.O. Box 217, 7500 AE Enschede, The Netherlands

a.torkabadi@utwente.nl

Abstract. It has been widely observed that below the yield stress the loading/unloading stress-strain curves of plastically deformed metals are in fact not linear but slightly curved, showing a hysteresis behaviour during unloading/reloading cycles. In addition to the purely elastic strain, extra dislocation based micro-mechanisms are contributing to the reversible strain of the material which results in the nonlinear unloading/reloading behaviour. This extra reversible strain is the so called anelastic strain. As a result, the springback will be larger than that predicted by FEM considering only the recovery of the elastic strain. In this work the physics behind the anelastic behaviour is discussed and experimental results for a dual phase steel are demonstrated. Based on the physics of the phenomenon a model for anelastic behaviour is presented that can fit the experimental results with a good accuracy.

1. Introduction

There has been an increasing interest by the automotive industry towards employing Advanced High Strength Steels (AHSS) in the past years. However the dimensional accuracy of the dual phase steel part remains an industrial issue [1]. In the past years most researches were focused on the development of novel plasticity models to give an accurate stress prediction. Nevertheless, little has been done in modeling the material behaviour during unloading upon release of the constraining force. The material behaviour upon unloading is of importance for the springback prediction considering that the experimental evidence shows that assuming a Hookean behaviour to describe the unloading is not realistic. It has been observed experimentally that the material shows a nonlinear unloading behaviour as well as reloading behaviour after being plastically deformed [2-4]. This is caused by an extra reversible strain recovered during unloading along with the pure elastic strain [5]. The root cause of this phenomenon is the short-range reversible movement of the dislocations known as anelasticity [6-8]. The dislocation structures which are impeded by the pinning points or piled up before the grain boundaries can move to a new equilibrium upon the relaxation of the lattice stress, contributing to some extra microscopic strain.

From an engineering perspective, considering that the total recovered strain during unloading governs the springback magnitude, it is essential to take into account the anelastic strain in the material models for the FEM springback simulations. In that respect, various researchers have adopted an approach attributed to E-modulus degradation [9-14]. In this approach the E-modulus of the material is made a function of the equivalent plastic strain in the simulations. Hence, the E-modulus represents the chord modulus which is measured from the experiments. The draw back with this approach is that it is assumed that all the points in the material are unloaded to the zero stress. This is not a realistic assumption in industrial forming processes. Therefore for a better springback prediction it is critical to model the nonlinear unloading behaviour. In this work by quantifying the anelastic strain, a model for describing the nonlinear unloading behaviour is proposed and the model prediction is compared with experimental data.

2. Constitutive modelling

The proposed model is based on the additive decomposition of the total strain increment into elastic $\dot{\boldsymbol{\varepsilon}}^{e}$, anelastic $\dot{\boldsymbol{\varepsilon}}^{an}$ and plastic $\dot{\boldsymbol{\varepsilon}}^{p}$ strain.

$$\dot{\boldsymbol{\varepsilon}} = \dot{\boldsymbol{\varepsilon}}^{e} + \dot{\boldsymbol{\varepsilon}}^{an} + \dot{\boldsymbol{\varepsilon}}^{p} \tag{1}$$

The rate of the elastic strain is given according to

$$\dot{\boldsymbol{\varepsilon}}^{e} = \overline{\boldsymbol{E}}^{-1}:\dot{\boldsymbol{\sigma}} \tag{2}$$

and the plastic strain rate is

$$\dot{\boldsymbol{\varepsilon}}^{p} = \dot{\lambda}\boldsymbol{N} \tag{3}$$

where $\boldsymbol{N}$ is the normal vector to the yield surface which depends on the derivative of the yield function at the end of the increment. The rate of the anelastic strain is given as

$$\dot{\boldsymbol{\varepsilon}}^{an} = \dot{\xi}\boldsymbol{N} \tag{4}$$

where ξ is the anelastic multiplier. It is assumed that the anelastic strain follows the normality condition and is co-directional with the plastic strain increment. This assumption originates from the physics of anelastic strain. The evolution of ξ is provided as [5]

$$\xi = \left(K\left(\sigma_f - \sigma_{y0}\right) + {\varepsilon_{pre}^{an}}^{0.5}\right)^2 \cdot g(s) \tag{5}$$

In the equation above, K is material related parameter obtained from experiment, σ_f is the flow stress of the material and can be described by a hardening law, σ_{y0} is the yield point of the material, ε_{pre}^{an} is the pre-yield anelastic strain and its value is determined from experiments. $g(s)$ is a function which describes the nonlinearity of the unloading/loading curves as a function of s. The variable s is a dimensionless stress dependent parameter which is defined as

$$s = \begin{cases} \sigma_{eq}/\sigma_f & if\ \varphi < 0\ and\ \boldsymbol{\sigma}:\dot{\boldsymbol{\sigma}} > 0 \\ 1 - \sigma_{eq}/\sigma_f & if\ \varphi < 0\ and\ \boldsymbol{\sigma}:\dot{\boldsymbol{\sigma}} < 0 \\ 1 & if\ \varphi \geq 0 \end{cases} \tag{6}$$

where σ_{eq} is the equivalent stress and φ is the yield function.
In order to describe the nonlinear behaviour of the anelastic strain, the $g(s)$ function is given as

$$g(s) = \sinh(\alpha.s^2)/\sinh(\alpha) \tag{7}$$

α is a constant whose value is determined from curve fitting to the experimental data.

There are numerous hardening models proposed in the literature relating the flow stress (σ_f) to the equivalent plastic strain (ε_{eq}^{p}). In this case, the Swift hardening law is used according to

$$\sigma_f = C\left(\varepsilon_0 + \varepsilon_{eq}^{p}\right)^n \tag{8}$$

From Equation (5), (6) and (8) the rate of the anelastic multiplier can be written as

$$\dot{\xi} = \frac{\partial \xi}{\partial \boldsymbol{\sigma}}:\dot{\boldsymbol{\sigma}} + \frac{\partial \xi}{\partial \lambda}\dot{\lambda} \tag{9}$$

Correspondingly, the rate of the anelastic strain is

$$\dot{\boldsymbol{\varepsilon}}^{an} = \left(\frac{\partial \xi}{\partial \boldsymbol{\sigma}}:\dot{\boldsymbol{\sigma}} + \frac{\partial \xi}{\partial \lambda}\dot{\lambda}\right)\boldsymbol{N} \tag{10}$$

Combining Equation (1), (2), (3) and (10) yields

$$\dot{\boldsymbol{\varepsilon}} = \overline{\boldsymbol{E}}^{-1}:\dot{\boldsymbol{\sigma}} + \dot{\xi}\boldsymbol{N} + \dot{\lambda}\boldsymbol{N} \tag{11}$$

The value of each strain is evaluated simultaneously through an implicit algorithm. The set of residual functions for every increment at the i[th] iteration is elaborated as

$$\boldsymbol{R}_{\sigma}^{i} = \Delta\boldsymbol{\varepsilon} - \overline{\boldsymbol{E}}^{-1}:\Delta\boldsymbol{\sigma} - \Delta\xi\boldsymbol{N} - \Delta\lambda\boldsymbol{N} \tag{12}$$

$$R_\lambda^i = -\varphi \tag{13}$$

The linearization yields

$$\begin{bmatrix} \dfrac{\partial \boldsymbol{R}_\sigma^i}{\partial \boldsymbol{\sigma}} & \dfrac{\partial \boldsymbol{R}_\sigma^i}{\partial \lambda} \\ \dfrac{\partial R_\lambda^i}{\partial \boldsymbol{\sigma}} & \dfrac{\partial R_\lambda^i}{\partial \lambda} \end{bmatrix} \begin{bmatrix} \delta\boldsymbol{\sigma} \\ \delta\lambda \end{bmatrix} = \begin{bmatrix} \boldsymbol{R}_\sigma^i \\ R_\lambda^i \end{bmatrix} \tag{14}$$

At the end of every iteration, the stress and plastic multiplier is updated by $\delta\boldsymbol{\sigma}$ and $\delta\lambda$ until the norm of the residual vector is smaller than the accepted tolerance.

3. Experimental

In order to determine the parameters for the anelastic model, cyclic uniaxial loading / unloading / reloading experiments were conducted on a DP800 steel with a thickness of 1. In such experiments the material was loaded to certain force and then unloaded to zero force. In the subsequent cycles the loading force was increased incrementally. The schematic illustration of the experimental procedure is shown in Figure 1.

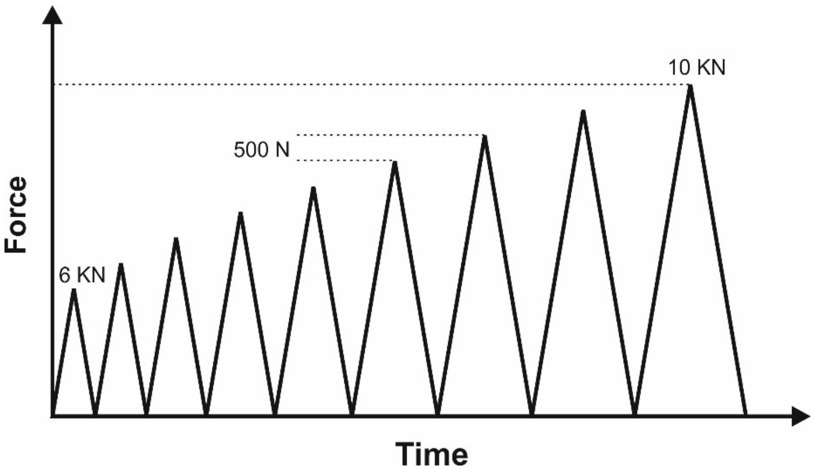

Figure 1. Schematic illustration of the experimental procedure.

From such experiments the material parameters for Swift hardening law and the anelastic model were obtained. Table 1 summarizes the material parameters obtained from experimental data to calibrate the Swift hardening and anelastic model.

Table 1. Material parameters.

$\sigma_f = C\left(\varepsilon_0 + \varepsilon_{eq}^p\right)^n$			$\xi = \left(K\left(\sigma_f - \sigma_{y0}\right) + {\varepsilon_{pre}^{an}}^{0.5}\right)^2 (\sinh(\alpha.s^2)/\sinh(\alpha))$			
$C\ (MPa)$	ε_0	n	$K(MPa^{-1})$	$\sigma_{y0}\ (MPa)$	ε_{pre}^{an}	α
1710	0.0072	0.28	5.1 x 10^{-5}	430	3 x 10^{-4}	0.68

4. Results and discussion

In Figure 1(a) the stress-strain curves obtained from the cyclic loading / unloading / reloading experiment and the curve predicted by the Swift + anelastic models are compared. For a better comparison, the zoomed in view of the 7th unloading/reloading cycle is shown in Figure 1(b). Besides, the unloading curves predicted by the E-modulus ($E = 210\ GPa$) and the chord modulus ($E_c = 164\ GPa$) are shown in Figure 1(b).

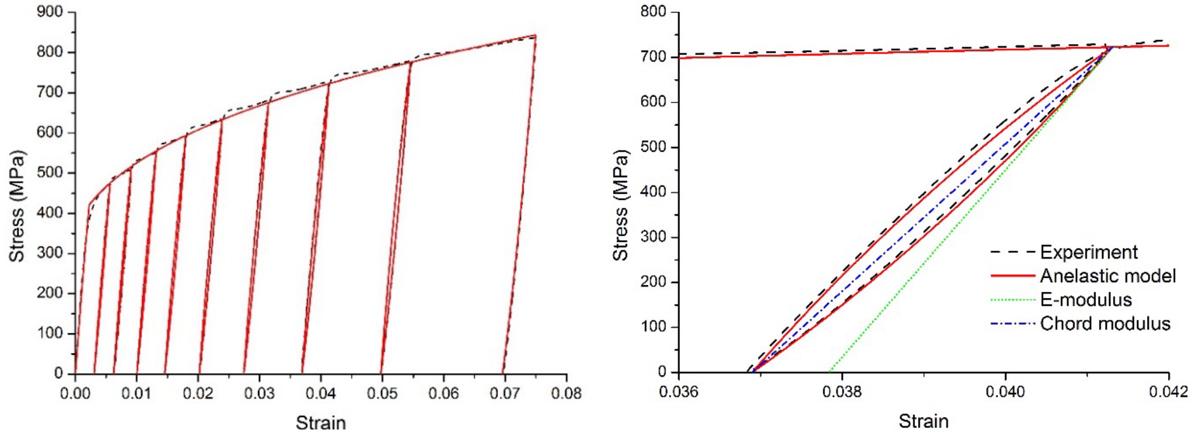

(a) (b)

Figure 2. Stress-strain response of DP800 (a) model prediction (red) and experimental data (black); (b) the magnified view of the 7th unloading/reloading cycle.

In Figure 1(b) it can be seen that predicting the unloading strain using the E-modulus can result in a large deviation from the material behaviour. The unloading behaviour approximated by the chord modulus is closer to reality; however, it is accurate only if it is assumed that all the parts in the material are unloaded to zero stress. Yet, the unloading curve predicted by the proposed anelastic model provides a good prediction through the whole unloading curve capturing the nonlinear behaviour.

5. Conclusion

In this study a model was proposed to capture the nonlinear unloading / reloading behaviour in AHSS. The model was calibrated to the experimental data obtained from DP800 steel using cyclic unloading / reloading experiments. To that end, four parameters were fitted to the experimental data. A comparison between the experimental results and the model shows a good correlation for the whole unloading / reloading path. Hence, using the proposed model in FEM simulations of forming processes will result in better prediction of the springback behaviour of complex parts.

References

[1] Wagoner R H, Lim H, and Lee M-G, *Advanced Issues in springback.* International Journal of Plasticity, 2013. **45**(0): p. 3-20.

[2] Cleveland R M and Ghosh A K, *Inelastic effects on springback in metals.* International Journal of Plasticity, 2002. **18**(5–6): p. 769-785.

[3] Eggertsen P A, Mattiasson K, and Hertzman J, *A Phenomenological Model for the Hysteresis Behavior of Metal Sheets Subjected to Unloading/Reloading Cycles.* Journal of Manufacturing Science and Engineering, 2011. **133**(6): p. 061021-061021.

[4] Sun L and Wagoner R H, *Complex unloading behavior: Nature of the deformation and its consistent constitutive representation.* International Journal of Plasticity, 2011. **27**(7): p. 1126-1144.

[5] Torkabadi A, van Liempt P, Meinders V T, and van den Boogaard A H. *A constitutive model for the anelastic behavior of Advanced High Strength Steels*. in *COMPLAS XIII*. CIMNE.

[6] Zener C M and Siegel S, *Elasticity and Anelasticity of Metals.* The Journal of Physical and Colloid Chemistry, 1949. **53**(9): p. 1468-1468.

[7] Ghosh A K, *A physically-based constitutive model for metal deformation.* Acta Metallurgica, 1980. **28**(11): p. 1443-1465.

[8] van Liempt P and Sietsma J, *A physically based yield criterion I. Determination of the yield stress based on analysis of pre-yield dislocation behaviour.* Materials Science and Engineering: A, 2016. **662**: p. 80-87.

[9] Morestin F and Boivin M, *On the necessity of taking into account the variation in the Young modulus with plastic strain in elastic-plastic software*. Nuclear Engineering and Design, 1996. **162**(1): p. 107-116.
[10] Li X, Yang Y, Wang Y, Bao J, and Li S, *Effect of the material-hardening mode on the springback simulation accuracy of V-free bending.* Journal of Materials Processing Technology, 2002. **123**(2): p. 209-211.
[11] Yoshida F, Uemori T, and Fujiwara K, *Elastic–plastic behavior of steel sheets under in-plane cyclic tension–compression at large strain.* International Journal of Plasticity, 2002. **18**(5–6): p. 633-659.
[12] Yang M, Akiyama Y, and Sasaki T, *Evaluation of change in material properties due to plastic deformation.* Journal of Materials Processing Technology, 2004. **151**(1–3): p. 232-236.
[13] Fei D and Hodgson P, *Experimental and numerical studies of springback in air v-bending process for cold rolled TRIP steels.* Nuclear Engineering and Design, 2006. **236**(18): p. 1847-1851.
[14] Yu H Y, *Variation of elastic modulus during plastic deformation and its influence on springback.* Materials & Design, 2009. **30**(3): p. 846-850.